Journal of Neuropathology and Experimental Neurology

Vol. 56, No. 2
February, 1997
pp. 143–149

Microglial Cell Activation in Aging and Alzheimer Disease: Partial Linkage with Neurofibrillary Tangle Burden in the Hippocampus

PIER LUIGI DIPATRE, MD AND BENJAMIN B. GELMAN, MD, PHD

Abstract. Microglial cells are the main component of the brain's resident immune system and are activated in Alzheimer disease (AD). We quantified the density of activated microglial cells (AMG) in 8 sectors of human hippocampus to determine if their density is correlated with senile plaque (SP) and neurofibrillary tangle (NFT) formation. Ferritin-stained microglia, Bielschowsky-stained neuritic plaques, and perikarya containing NFTs were counted in 8 young adults, 9 nondemented elderly adults, and 9 demented patients with AD. Microglial cell activation was moderately higher in elderly nondemented subjects. In AD there was a more striking activation in all sectors of the hippocampus. Most AMGs were distributed diffusely in neuropil and were not delimited to SPs or NFTs. Senile plaque counts were not linked with AMG counts within any sector. Neurofibrillary tangle counts were correlated significantly with AMG counts within one sector, the subiculum. When variations within and between sectors were factored out statistically, the burden of AMGs was correlated significantly with the burden of NFTs ($r = 0.34$; $p < 0.005$), but not SPs. Neuropathologic changes at the origin of the perforant pathway were correlated significantly with orthograde microglial cell activation in the termination field. These observations show that correlations between microglial cell activation and pathologic features of AD are only rarely significant. When significant linkage was present, it involved NFTs and not SPs, and depended on which sector of hippocampus was examined.

Key Words: Aging; Alzheimer disease; Hippocampus; Microglial cell; Neurofibrillary tangle.

INTRODUCTION

Theories on the pathophysiology of Alzheimer disease (AD) have focused on the composition of 2 distinguishing neuropathological features: senile plaques (SP) and neurons containing neurofibrillary tangles (NFT) (1). Because activated microglial cells are found within senile plaques, it has been suggested that immune activation may play a role in SP formation and AD pathogenesis (2, 3). Microglial cells in senile plaques usually exhibit a phenotype distinct from resting microglia, appearing hypertrophic with thick, highly ramified processes (4, 5). Class II histocompatibility antigen (HLA-DR) expression is high in microglial cells near amyloid deposits in senile plaques (6–10). Microglia in AD also express high levels of MHC class I receptors (8), C1q and C3 (11), interleukin-1 (12), and ferritin (13–19), providing strong evidence for phenotypic activation. Activated mononuclear phagocytes can secrete potentially neurotoxic cytokines, and it has been proposed that microglial cell activation may participate actively in the formation of senile plaques in AD (2, 5, 8, 12, 20, 21). One proposal is that excessive deposition of the β-amyloid precursor protein (βA) induces activation of microglial cells which secrete IL-1, driving the progression to neuritic (senile) plaques (12). Treatment of cultured microglia with βA leads to secretion of tumor necrosis factor α and nitric oxide; both are potential neurotoxins, suggesting another mechanism for exacerbation of SP formation (22, 23). Results from some clinical trials have suggested that treatment with anti-inflammatory drugs may delay the onset of dementia in AD (20). These results have been interpreted to suggest that brain inflammatory cells can exert detrimental effects clinically (2). Still, it remains difficult to exclude the possibility that the microglia are an epiphenomenon in AD with no detrimental pro-inflammatory effects.

If the microglia contribute significantly to the neuropathologic changes of AD, then vulnerable regions of brain tissue would be likely to exhibit more intense microglial cell activation. The hippocampus is an ideal structure for performing a regional analysis because SPs and NFTs appear there early in the course of AD, and there is an uneven distribution across sectors (24). A further advantage of mapping the hippocampus is that knowledge of the intrahippocampal circuitry is available, affording insights into transaxonal connections between spatially separate sectors (25). Here we have mapped the density of activated microglial cells in sectors of the human hippocampus and have compared them to densities of SPs and NFTs within, between, and across sectors. A portion of the results were presented in a preliminary communication (26).

MATERIALS AND METHODS

Subjects

Formalin-fixed, paraffin-embedded brains obtained at autopsy from 3 groups of patients were examined. (a) Nine clinically demented subjects with a histopathological diagnosis of AD using CERAD-defined criteria (27) (mean age 72 years); (b) Nine age-matched nondemented control subjects (mean age 73 years) with no neuropathologic abnormality; (c) Eight young adult controls without any neuropathologic abnormality (mean age 38 years). To qualify for inclusion in the study, the control

From the Departments of Pathology (PLD, BBG) and Anatomy and Neurosciences (BBG), the University of Texas Medical Branch 0785, Galveston, TX 77550.

Correspondence to: Benjamin B. Gelman, MD, PhD, the Department of Pathology, 0785, the University of Texas Medical Branch, Galveston, TX 77550.

subjects selected had no histologic evidence of acute neuronal necrosis of hippocampal neurons. The causes of death in the elderly nondemented controls were (number of subjects in brackets): malignant neoplasm [4], acute shock [2], renal failure [1], emphysema [1], and pneumonia [1]. The causes of death in the young adult controls were: malignant neoplasm [2], liver failure [2], acute shock [3], and drowning [1]. Mean time intervals between death and the postmortem examination did not differ between groups, and was not a significant independent variable in multiple regression models (described below).

Tissue Staining

Blocks of midhippocampus at the level of the lateral geniculate body were obtained after fixation of whole brains for 2 weeks in buffered 10% formalin. After dehydration and embedding in paraffin, 7-micron-thick tissue sections were mounted on poly-L-lysine-coated glass slides. Ferritin immunohistology was used to visualize activated microglia, an approach used in several previous studies of AD (13–19). Deparaffinized sections were immersed sequentially in polyclonal rabbit anti-human ferritin (Boehringer-Mannheim, Indianapolis, IN), biotinylated antirabbit IgG, and avidin-biotin complex (ABC, Vector Laboratories, Carpenteria, CA) (19, 28, 29). Nuclei were counterstained with Mayer's hematoxylin. Immunostaining for all 26 patients was performed in a single batch. Neurofibrillary tangles and SPs were visualized using Sevier and Munger's modified Bielschowsky silver stain (30).

Quantification

Regions of hippocampus individually analyzed were: layers 2 and 3 and 4 and 5 of the entorhinal cortex (E3 and E5), which are enriched with NFTs and SPs; the 4 subdivisions of Ammon's horn (C1, CA2, CA3, and CA4); subiculum; and the molecular layer of the dentate gyrus. Counting was performed without knowledge of the identity of the subject using a 40x objective in a minimum of 10 microscopic fields (0.17 mm^2) per sector (29). Field selection was performed beginning in CA4 and counting consecutive fields, first on one side of Ammon's horn, advancing forward to the center, advancing forward to opposite edge of Ammon's horn, and then repeating these side-to-side forward sweeps. The stage was advanced in this way along the entire length of the molecular layer until the neocortex was reached. In the case of the dentate gyrus, both inner and outer molecular layers were surveyed in contiguous fields. Results are given as mean objects per unit field area (units/mm^2). Using this method, numbers of SPs and neurons containing NFTs in each region were counted in Bielschowsky-stained sections. Stained extracellular tangles were not tallied because they were not abundant enough to analyze separately using the design and statistical methods of the study. In subserial sections, ferritin-stained microglial cells that had stained cytoplasmic processes and contained a nucleus in the plane of section were tallied (29). If a field contained stained microglia within a SP, these cells were counted (i.e. the contribution of SPs to the overall density of activated microglia was included in the tally).

Statistical Analysis

Group effects within and between sectors of the hippocampus were evaluated using the Student's t test, one-way analysis of variance, or both. Linear correlation coefficients were calculated for each dependent variable within and between hippocampal sectors (31). A multiple regression model (32) was constructed using activated microglial cell density as the dependent variable and these potential independent variables: sector of hippocampus; density of senile plaques; density of neurons containing NFTs; postmortem time interval. Variables were first screened using forward selection and statistical significance was confirmed using backward elimination at a P value of 0.05.

RESULTS

Appearance and Distribution of Microglia in Nondemented Controls

Ferritin-stained microglial cells in young control subjects were sparse (Fig. 1A); their appearance was characterized by a few thin immunostained processes and slight perinuclear staining, consistent with resting microglia. The microglia in elderly controls (Fig. 1B) were more numerous and were more heavily stained. Their stained processes were often thickened and had branching networks, morphologic features of activation. Compared to young adults, the elderly control subjects exhibited a statistically significant increase in the density of activated microglial cells in all 8 sectors studied (Fig. 2). There was substantial variation from sector to sector, with the greatest increase (2.36x) occurring in CA2 (Fig. 3).

Appearance and Distribution of Microglia in Alzheimer Disease

There was a very striking increase in the density of stained microglial cells in all the patients with AD. The majority of stained cells were distributed diffusely in the neuropil (Fig 1C). Patients with AD had significantly more microglial cells than elderly control patients in all sectors examined (Figs. 2, 3). Microglial cell processes were much more numerous and thickened compared to elderly and young controls, consistent with marked activation (Fig. 1). Senile plaques contained microglial cells (14–18), but the preponderance of stained cells were distributed diffusely in the neuropil. Increased microglia in AD were distributed evenly across sectors of hippocampus (Fig. 3) and the sector containing the most pronounced increase was the subiculum (vs CA2 in baseline aging).

Microglia and AD Neuropathology within Sectors

In subjects with AD, densities of SPs and NFTs exhibited substantial variation from sector to sector (Table 1). These regional variations are comparable to results obtained in previous studies (33). Overall, the density of microglia within a given sector of the hippocampus showed little linkage with SP density. Linear regression analysis confirmed that the density of activated microglial cells did not correlate significantly with SP density within any sector (Table 2). The density of NFTs did, however,

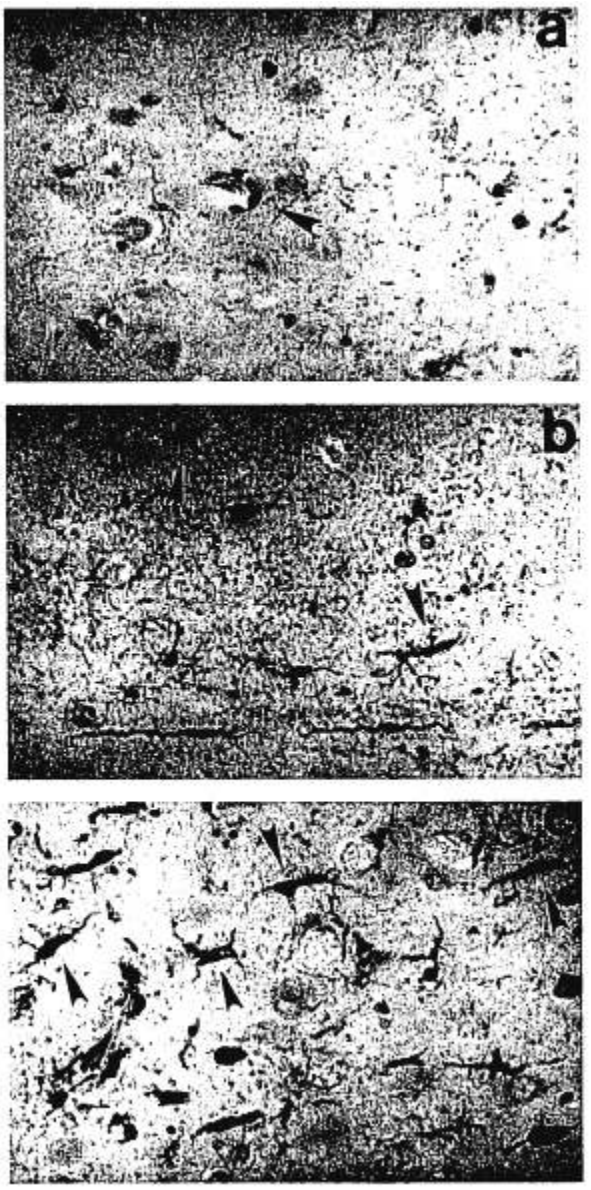

Fig. 1. Ferritin-stained microglial cells in hippocampus CA1 sector of a 36-year-old adult (a), a 77-year-old nondemented subject (b), and a 73-year-old demented patient with Alzheimer disease (c). All panels are shown at the same magnification and were processed in a single batch. Stained microglia (examples marked by arrowpoints) in the young adult are sparse. In the elderly nondemented control they are more prevalent; note the elongated bipolar microglia at the bottom of this field. In the demented patient they are sharply increased in number and display more complex ramified processes, typical of activation. ×200.

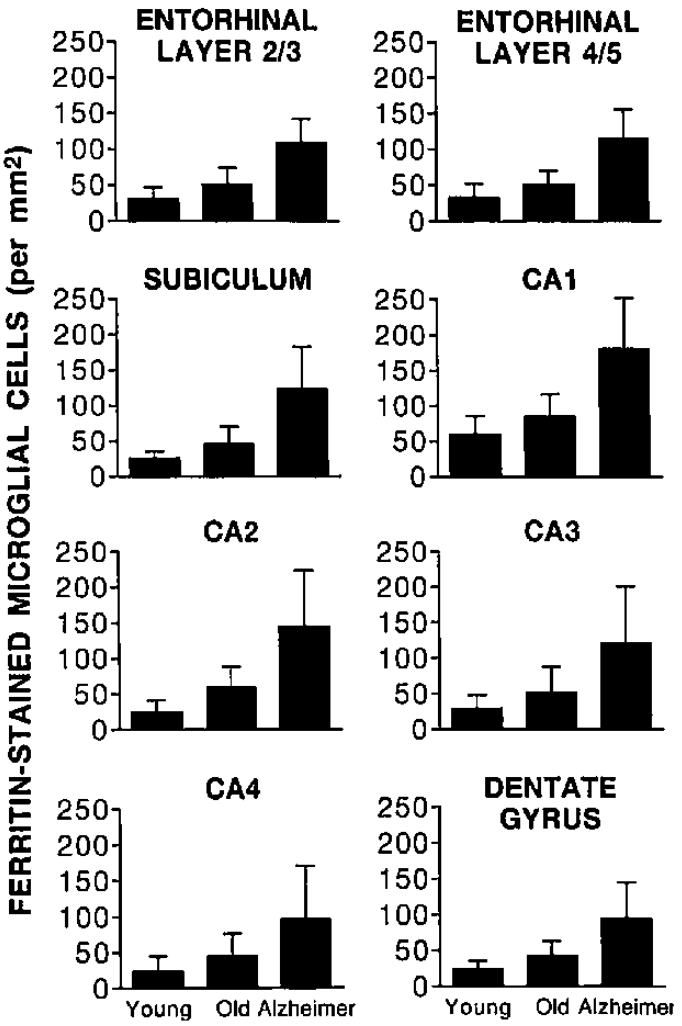

Fig. 2. Density of ferritin-stained microglial cells in 8 sectors of the hippocampus (± 1 standard deviation). The increase in the elderly controls compared to young controls was statistically significant in all sectors ($p < 0.01$). The increase in Alzheimer disease compared to elderly controls was significant in all sectors ($p < 0.001$).

correlate significantly with microglial cell activation in 1 out of 8 sectors, the subiculum (Table 2).

Microglia and AD Neuropathology between Sectors

An advantage of mapping the hippocampus is that knowledge of the intrahippocampal circuitry is available (25). This information permitted us to ask if there is linkage between microglia across spatially-separate, but functionally connected sectors. Interconnected sectors showed few ties between microglia and AD pathology, but there was a notable exception (Table 3). The density of SPs at the origin of the perforant pathway (EC 2/3) correlated with microglial activation at its termination in the outer molecular layer of the dentate gyrus. No other significant between-sector correlations with SPs were present. The same analysis performed between NFTs and microglia contained no significant correlations (data not presented).

Microglia and AD Neuropathology across Sectors

Microglia are mobile and their localization is potentially dynamic. At autopsy their spatial distribution may not be synchronized with the evolution of pathological

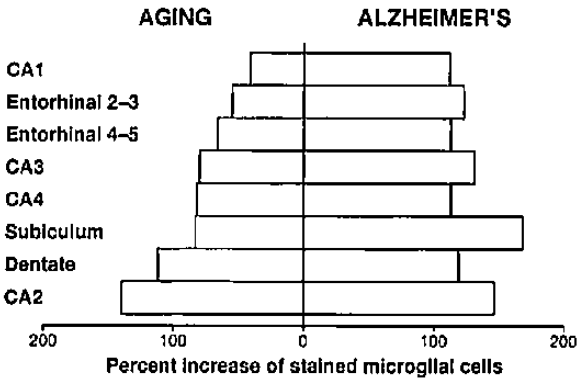

Fig. 3. Increased density of stained microglial cells in 8 sectors of hippocampus. The incremental increase caused by baseline aging (left bars) is compared to the incremental increase caused by Alzheimer disease (right bars). For aging, the percentage shown is for old controls relative to young nondemented controls. For Alzheimer disease the percentage shown is for elderly AD subjects relative to age-appropriate elderly controls.

TABLE 1
Distribution of Senile Plaques and Neurofibrillary Tangles in the Hippocampus

Region of hippocampus	Subjects	Neuritic plaques per mm²	Perikarya with NFTs per mm²
Entorhinal cortex layers 2 and 3	9	23.7 ± 14.2	44.7 ± 46.4
Entorhinal cortex layers 4 and 5	9	13.8 ± 15.2	37.8 ± 32.0
Subiculum	9	6.9 ± 5.8	27.6 ± 25.3
Ammon's horn, CA1	9	13.1 ± 9.3	57.1 ± 34.3
Ammon's horn, CA2	8	10.2 ± 8.8	49.9 ± 32.9
Ammon's horn, CA3	7	1.8 ± 2.3	5.4 ± 6.3
Ammon's horn, CA4	8	1.3 ± 1.9	4.2 ± 3.5
Dentate gyrus, outer molecular	9	8.1 ± 4.1	—

changes or severity of dementia. Thus, it is possible that overall burdens of microglial cells, SPs, and NFTs are linked in ways that do not depend upon co-concentration within sectors. To address the question of spatial congruency, we isolated the influence of variations between sectors using multiple regression analysis. Factoring out variations from sector to sector, the results showed a substantial and statistically significant correlation between microglial cells and NFT burdens across sectors of the hippocampus (Table 4). No similar linkage with SP density was present in this regression model.

DISCUSSION

The main issue addressed here is whether there is spatial congruency or numeric correlation between immune cell activation and the main pathologic feature of AD,

TABLE 2
Correlation between Microglial Cell Activation and Alzheimer Disease Neuropathology within Hippocampal Sectors

Region of hippocampus	Correlation coefficients between microglial cell density and: Plaque density	Tangle density
Entorhinal cortex layers 2 and 3	0.1440	0.3613
Entorhinal cortex layers 4 and 5	0.5211	0.5411
Subiculum	0.0469	0.8187*
CA1	0.3591	0.2666
CA2	0.0255	0.1433
CA3	0.3098	0.0505
CA4	0.4941	0.1903
Dentate gyrus	0.2445	—

* $p < 0.005$; least squares regression.

senile plaques. We found that sectors of hippocampus containing the most senile plaques did not exhibit more intense microglial cell activation. Low SP counts were accompanied by a high density of activated microglia in some cases. Concentration within or near SPs, stressed in some previous studies (2, 10, 12, 14, 21), was overshadowed by the diffuse nature of the process. When the density of activated microglia was high, they were usually located in vast areas of neuropil between SPs. The hypothesis that spatial variations in SP density parallels that of activated microglia is, therefore, contradicted by our observations. The pattern of microglial cell activation we observed in the neuropil, not restricted to SPs, has been increasingly emphasized in more recent studies (4, 5, 19).

Potential inducers of microglial cell activation include the loss of synapses, NFT degradation, axonal degeneration, and nonstructural anomalies (34). Our data showed a significant relationship with numbers of intracellular NFTs in one sector of the hippocampus. Despite the apparent specificity for subiculum, which remains unexplained, these data are the first quantitative evidence for linkage between microglia and intracellular NFTs. NFTs are more closely related to the clinical severity of dementia than SPs (35). Thus, the role of microglia in clinical progression of dementia needs to be given increased consideration. The anatomic location for future neuropathologic study should be chosen carefully. At autopsy, microglia and NFTs were co-concentrated only within the subiculum, making this sector a preferred site to probe their relationship.

The present data also revealed that microglial cell activation is significantly related to the neuropathologic changes of AD in a manner not dependent on co-concentration within sectors. A multiple regression model containing sector, SP density, and NFT density showed that only NFT density correlated significantly

TABLE 3
Microglial Cell Activation and Senile Plaque Density between Hippocampal Sectors

Hippocampal circuit	Origin of projections	Termination field	Correlation between: Microglial cells at origin vs SPs at termination	Correlation between: SPs at origin vs microglial cells at termination
Perforant pathway	Entorhinal cortex (2–3)	Dentate gyrus[a]	r = 0.2050 p = 0.5970	r = 0.6475 p = 0.0370*
Mossy fiber	Dentate gyrus	CA3	r = 0.0532 p = 0.9100	r = 0.1447 p = 0.7570
Schaffer collateral	CA3	CA1	r = −0.3642 p = 0.4220	r = −0.2648 p = 0.5660
Other	CA1	Subiculum	r = 0.4315 p = 0.2460	r = 0.1123 p = 0.7740
Other	Subiculum	Entorhinal cortex 4–5	r = 0.2687 p = 0.4850	r = 0.4263 p = 0.2530

[a] Dentate gyrus = outer molecular layer; SP = senile plaque; r = Pearson's correlation coefficient; * = statistically significant.

TABLE 4
Multiple Regression Model of Microglial Cell Activation and Alzheimer's Disease Neuropathology in Nine Subjects

Independent variables in regression model[a]	Dependent variable	Partial correlation (R)	Regression weight (ß)	p value
Sector of hippocampus[b]	Microglial cell density	0.034	0.037	0.272
Senile plaque density		0.047	0.052	0.707
Neurofibrillary tangle density		0.342	0.396	0.005*

[a] Multiple R = 0.4070; p = 0.009; n = 67.
[b] Sectors of hippocampus included in model: entorhinal cortex layers 2 and 3 and 4 and 5, subiculum, CA1, CA2, CA3, CA4, and dentate gyrus outer molecular layer.

with the burden of microglial cells ($p < 0.005$). In essence, this curious result says that the numbers of microglia and NFTs are linked, but rarely are they restricted to the same sector of hippocampus. The correlation provides only modest predictive power in a single patient ($r^2 = 0.12$), but it stands in stark contrast to the lack of linkage with SP burden. Microglia have been previously associated with extracellular tangles (36, 37), but an association with intracellular tangles has not been emphasized previously. There are many possible reasons why microglia and NFT burdens rarely overlap within sectors. The temporal evolution of NFT formation may have a different chronology, overlapping weakly with microglial cell responses. Microglial cell mobility (38) also could have an influence because their location at autopsy might not coincide with sites of old structural damage. The two anomalies could be influenced by an underlying neurotrophic factor that is distributed unevenly in the hippocampus. All these factors could obscure contacts occurring earlier in the disease process. Finally, and perhaps most importantly, sectors with a paucity of microglia could harbor caches of key subpopulations; enrichment with a crucial phenotype could have important effects even when the total cell count is low.

Our experimental paradigm permitted us to evaluate another relevant issue previously raised in the literature. Microglial cell activation is one response to transsynaptic or transaxonal degenerations orthograde or retrograde to foci of degeneration (34). This suggests that microglial cell activation in one sector could be related to pathologic changes in a functionally connected, but spatially separate sector. We found a relationship of this type in the perforant pathway, where the number of senile plaques at the origin was linked statistically with the number of microglia in the termination field (Table 3). Many other anomalies have been observed in the terminal zone of the perforant pathway, including loss of synaptic protein, synaptic plasticity, decreased glutamate, and decreased glucose transporter protein (39). Hyman and associates have suggested that loss of cortical-hippocampal feedforward projections in AD causes orthograde anomalies in crucial memory circuits (39, 40). The present data support that concept, adding microglial cell activation to the list of responses to deafferentation. Whether or not microglial cell activation correlates with the other anomalies previously described in the perforant pathway is an interesting problem for future study.

We tested a final hypothesis: that the impetus for microglial cell activation in AD is derived from an accelerated aging sequence (33). The regional pattern of immune activation between sectors of the hippocampus did not resemble the pattern in normal aging. Activation in aging was highly variable between sectors and was most pronounced in CA2; in AD there was little variation between sectors and the increase was highest in the subiculum (Fig. 3). Thus, our data make it unlikely that immune activation in AD is a simple exaggeration or intensification of the normal pattern of degeneration in the aging hippocampus.

Quantitative regional analysis of microglial cell activation in the hippocampus of patients with AD has yielded these new observations: (a) Correlations with senile plaque densities were not significant. (b) There was linkage with burden of neurofibrillary tangles, but the only sector in which linkage was close enough for more detailed morphologic study was the subiculum. (c) There was little similarity with the spatial pattern associated with baseline aging. (d) In the perforant pathway activation may in part be a response to deafferentation. Microglial cell activation probably plays multiple and possibly divergent roles in the disease process (19). NFT density accounted for only a small proportion of the variation; other anomalies, such as loss of synaptic density (41), could provide a more important substrate for immune activation. Thus, whether or not microglia promote pathologic changes leading to dementia remains an important issue with intriguing therapeutic implications.

REFERENCES

1. Perry G, Smith MA. Senile plaques and neurofibrillary tangles: What role do they play in Alzheimer's disease? Clin Neurosci 1993;1:199–203
2. McGeer PL, Walker DG, Akiyama H, Yasuhara O, McGeer EG. Involvement of microglia in Alzheimer's disease. Neuropathol Appl Neurobiol 1994;20:191–92
3. Kalaria RN. Cerebral microvasculature and immunological factors in Alzheimer's disease. Clin Neurosci 1993;1:204–11
4. Masliah E, Mallory M, Hansen L, et al. Immunoreactivity of CD45, a protein phosphotyrosine phosphatase, in Alzheimer's disease. Acta Neuropathol 1991;83:12–20
5. Carpenter AF, Carpenter, PW, Markesbery WR. Morphometric analysis of microglia in Alzheimer's disease. J Neuropathol Exp Neurol 1993;52:601–8
6. McGeer PL, Itagaki S, Tago H, McGeer EG. Reactive microglia in patients with senile dementia of the Alzheimer type are positive for the histocompatibility glycoprotein HLA-DR. Neurosci Lett 1987;79:195–200
7. Mattiace LA, Davies P, Dickson DW. Detection of HLA-DR on microglia in the human brain is a function of both clinical and technical factors. Am J Pathol 1990;136:1101–14
8. Tooyama T, Kimura H, Aiyama H, McGeer PL. Reactive microglia express class I and class II major histocompatibility complex antigens in Alzheimer's disease. Brain Res 1990;523:273–80
9. Styren SD, Civin WH, Rogers J. Molecular, cellular, and pathologic characterization of HLA-DR immunoreactivity in normal elderly and Alzheimer's disease brain. Exp Neurol 1990;110:93–104
10. Perlmutter LS, Scott SA, Barron E, Chui HC. MHC class II-positive microglia in human brain: Association with Alzheimer lesions. J Neurosci Res 1992;33:549–58
11. Johnson SA, Lampert-Etchells M, Pasinetti GM, Rpzovsky I, Finch CE. Complement mRNA in the mammalian brain: Responses to Alzheimer's disease and experimental brain lesioning. Neurobiol Aging 1992;13:641–48
12. Griffin WST, Sheng JG, Roberts GW, Mrak RE. Interleukin- 1 expression in different plaque types in Alzheimer's disease: Significance in plaque evolution. J Neuropathol Exp Neurol 1995;54:276–81
13. Jellinger K, Paulus W, Grunke-Iqbal I, Riederer P, Youdim MB. Brain iron and ferritin in Parkinson's and Alzheimer's diseases. J Neural Transm Park Dis Dement Sect 1990;2:237–40
14. Grundke-Ikbal I, Fleming J, Tung YC, Lassmann H, Iqbal K, Joshi JG. Ferritin is a component of the neuritic (senile) plaque in Alzheimer dementia. Acta Neuropathol 1990;81:105–10
15. Ohgami T, Kitamoto T, Shin RW, Kaneko Y, Ogomori K, Tateishi J. Increased senile plaques without microglia in Alzheimer's disease. Acta Neuropathol 1991;81:242–47
16. Miyazono M, Iwaki T, Kitamoto T, Kaneko Y, Doh-ura K, Tateishi J. A comparative immunohistochemical study of kuru and senile plaques with a special reference to glial reactions at various stages of amyloid plaque formation. Am J Pathol 1991;139:589–98
17. Connor JR, Menzies SL, St Martin SM, Mufson EJ. A histochemical study of iron, transferrin and ferritin in Alzheimer's diseased brains. J Neurosci Res 1992;31:75–83
18. Gelman BB. Iron in CNS disease. J Neuropathol Exp Neurol 1995;54:477–86
19. Roe MT, Dawson DV, Hulette CM, Einstein G, Crain BJ. Microglia are not exclusively associated with plaque-rich regions of the dentate gyrus in Alzheimer's disease. J Neuropathol Exp Neurol 1996;55:366–71
20. McGeer PL, McGeer EG. Anti-inflammatory drugs in the fight against Alzheimer's disease. Ann NY Acad Sci 1996;777:213–20
21. Cras P, Kawai M, Siedlak S, et al. Neuronal and microglial involvement in beta-amyloid protein deposition in Alzheimer's disease. Am J Pathol 1990;137:241–46
22. Goodwin JL, Uemura E, Cunnick JE. Microglial cell release of nitric oxide by the synergistic action of beta-amyloid and IFN-gamma. Brain Res 1995;692:207–14
23. Meda L, Cassatella MA, Szendrei GI, et al. Activation of microglial cells by beta-amyloid protein and interferon-gamma. Nature 1995;374:647–50
24. Braak H, Braak E. Neuropathological staging of Alzheimer's disease changes. Acta Neuropathol 191;82:239–59
25. Samuel W, Masliah E, Hill LR, Butters N, Terry R. Hippocampal connectivity and Alzheimer's dementia: Effects of synapse loss and tangle frequency in a two component model. Neurology 1994;44: 2081–88
26. DiPatre PL, Gelman BB. Hippocampal microglial cell activation is not correlated with plaque and tangle densities in Alzheimer's disease. Lab Invest 1995;72:135A
27. Mirra SS, Hart MN, Terry RD. Making the diagnosis of Alzheimer's disease. A primer for practicing pathologists. Arch Pathol Lab Med 1993;117:132–34
28. Gelman BB, Rodriguez-Wolf MG, Wen J, Kumar S, Campbell GA, Herzog N. Siderotic cerebral macrophages in the acquired immunodeficiency syndrome. Arch Pathol Lab Med 1992;116:509–16
29. Gelman BB. Diffuse microgliosis associated with cerebral atrophy in the acquired immunodeficiency syndrome. Ann Neurol 1993;34: 65–70
30. Sevier AC, Munger BL. A silver method for paraffin section of neural tissue. J Neuropathol Exp Neurol 1965;24:130–35

31. Remington RD, Schork MA. Statistics with applications to the biological and health sciences. Englewood Cliffs: Prentice-Hall, 1970:253–81
32. Darlington RB. Regression and linear models. New York: McGraw-Hill, 1990
33. Arriagada PV, Marzloff, Hyman BT. Distribution of Alzheimer-type pathologic changes in nondemented elderly individuals matches the pattern of Alzheimer's disease. Ann Neurol 1992;42:1681–88
34. Dickson DE, Mattiace LA, Kure K, et al. Microglia in human disease, with an emphasis on acquired immune deficiency syndrome. Lab Invest 1991;64:135–56
35. Arriagada PV, Growdon JH, Hedley-White ET, Hyman BT. Neurofibrillary tangles but not senile plaques parallel the duration and severity of Alzheimer's disease. Neurology 1992;42:631–39
36. Cras P, Kawai M, Siedlak S, Perry G. Microglia are associated with the extracellular neurofibrillary tangles of Alzheimer disease. Brain Res 1991;558:312–14
37. Ikeda K, Akyiama H, Haga C, Haga S. Evidence that neurofibrillary tangles undergo glial modification. Acta Neuropathol 1992;85:101–4
38. Hickey WF, Kimura H. Perivascular microglial cells of the CNS are bone marrow derived and present antigen in vivo. Science 1988;239:290–92
39. Harr SD, Simonian NA, Hyman BT. Functional alterations in Alzheimer's disease: Decreased glucose transporter 3 immunoreactivity in the perforant pathway terminal zone. J Neuropathol Exp Neurol 1995;54:38–41
40. Hyman BT, Van Hoesen GW, Kromer LT, Damasio AR. Perforant pathway changes and the memory impairment in Alzheimer's disease. Ann Neurol 1986;20:472–81
41. Terry RD, Masliah E, Salmon DP, et al. Physical basis of cognitive alterations in Alzheimer's disease: Synapse loss is the major correlate of cognitive impairment. Ann Neurol 1991;30:572–80

Received September 10, 1996
Revision received October 28, 1996
Accepted October 28, 1996